NJC

Accepted Manuscript

This is an *Accepted Manuscript*, which has been through the Royal Society of Chemistry peer review process and has been accepted for publication.

Accepted Manuscripts are published online shortly after acceptance, before technical editing, formatting and proof reading. Using this free service, authors can make their results available to the community, in citable form, before we publish the edited article. We will replace this *Accepted Manuscript* with the edited and formatted *Advance Article* as soon as it is available.

You can find more information about *Accepted Manuscripts* in the Information for Authors.

Please note that technical editing may introduce minor changes to the text and/or graphics, which may alter content. The journal's standard Terms & Conditions and the Ethical guidelines still apply. In no event shall the Royal Society of Chemistry be held responsible for any errors or omissions in this *Accepted Manuscript* or any consequences arising from the use of any information it contains.

ROYAL SOCIETY OF CHEMISTRY

www.rsc.org/njc

NJC

RSCPublishing

LETTER

Double role of the hydroxy group for water dispersibility and luminescence of REF_3 (RE=Yb,Er,Tm) based mesocrystals

Cite this: DOI: 10.1039/c3nj00000x

Xiang-Hong He,[a, b] and Bing Yan[a, *]

Received 00th XXXXX 2013,
Accepted 00th XXXXX 2013

DOI: 10.1039/c3nj00000x

www.rsc.org/njc

Presently, how to effectively utilize the hydroxy group serving the photoluminescence of lanthanide-activated micro-/nano-phosphors remains a formidable challenge, as it usually reduces or even quenches the emission via the non-radiative depopulation of an excited state of lanthanide ions. Herein, we address this issue by investigating the dual role of hydroxy group for luminescence and water-dispersion of REF_3 (RE=Yb,Er,Tm) mesocrystals fabricated via an additive-free solvothermal route. These mesocrystals can easily be dispersed in water, producing a stable colloidal solution. Due to the presence of high energy -OH group on the surface, Er^{3+} doped YbF_3 mesocrystals exhibited NIR-to-NIR down-conversion luminescence but no NIR-to-visible upconversion emission upon radiation of 980 nm, suggesting these mesocrystals are expected to be used as telecommunication optical materials or fluorescent labels.

T Water-dispersibility is needed in the major fields of applications of nanophosphors, that is, in bioimaging, labeling, and bioassays. [1]. Unfortunately, in most reported cases, commonly used high quality lanthanide-ion-doped nanophosphors via thermolysis have no intrinsic aqueous solubility due to the strong hydrophobicity of the commonly used surface capping agents like oleic acid and oleylamine, which becomes a great drawback for biomedical research.[1,2] Postsynthesis surface modifications to render these hydrophobic nanoparticles dispersible in aqueous media such as ligand exchange, surface silanization, and polymer coating are time-consuming and may lead to aggregation.[1–3] Oxidation of the oleate capping agent to azelaic acid yields adventitious MnO_2, which is difficult to separate from the azelaic capped nanoparticles and reults in weak luminescence.[4] Despite the recent advances in the fabrication of hydrophilic lanthanide-doped nanoparticles using various procedures and a variety of capping agents, it has been a challenge to prepare water dispersible nanophosphors through a facile additive-free technique.

It is well known that hydroxy group (–OH) in lanthanide ion activated phosphors is primary centers of nonradiative transition which usually reduces or even quenches luminescence of activator center via multiphonon relaxation.[5] Therefore, removing –OH group in phosphors is believed to be essential for enhancing emission. In fact, the presence of –OH group can render nanoparticles dispersible in aqueous systems. However, to the best of our knowledge, manipulation of –OH group servicing the photoluminescence and aqueous dispersion has been much less well explored so far.

Rare-earths trifluorides are the most important host crystals for lanthanide-doped phosphors, providing suitable trivalent sites where can be easily substituted by other trivalent lanthanide ions without additional charge compensation.[6] Yb^{3+}-Er^{3+} ion-pair is an excellent sensitizer-activator showing both up-conversion and down-shifting luminescence upon radiation of 980 nm continue laser.[5a] However, upconversion leading to visible emissions (green and red region) usually greatly reduces infrared emission at 1.5 μm.[8] It is difficult to achieve up-conversion or down-shifting while simultaneously prohibit the rest emission for Yb^{3+}-Er^{3+} co-doped phosphors so far. In this work, hydrophilic REF_3 (RE=Yb,Er,Tm) mesocrystals as well as Er^{3+}/Ce^{3+} single or double doped analogues were prepared by organic-additive-free solvothermal method at relatively low temperature (120 °C). The dual role of –OH group on dispersion and luminescence of Er^{3+}-doped YbF_3 has been investigated.

FESEM and TEM images in Fig. 1 illustrates that all the as-prepared nanophosphors are composed of relatively uniform nano-plates with the length×width×height sizes of around 135×132×65 nm) for YbF_3, about 80×80×35 nm for ErF_3, and around 90×90×40 nm for TmF_3. TEM images also revealed that REF_3 (RE=Yb,Er,Tm) samples take on a rhombic plate shape, either lying flat on the face or standing on the edge. Enlarged TEM image exhibits that the surfaces of nano-plates are not smooth. Each of them is composed of

many nanoparticles and shows the loose and somewhat hollow structures. The comparability of morphologies and sizes resulted from the same orthorhombic phase and the similar lattice constants. Both FESEM and TEM images illustrated their novel structure characters, which are constructed from many nanoparticles and exhibited coarse surfaces. Especially, as shown in Fig. 1, the SAED pattern observed on a monodisperse REF_3 nano-plate exhibits sharp and periodic spots, revealing its remarkable single-crystal-like feature. According to Cölfen et al, the regular-shaped REF_3 (RE=Yb,Er,Tm) nano-plates in this work are actually typical mesocrystallines.[9] The rough surface pattern and attachment of nanoparticels suggest that these mesocrystals resulted from self-assembling of nanoparticle subunits rather than the classic crystal growth.[9]

X-ray diffraction (XRD) patterns of as-prepared REF_3 (RE=Yb,Er,Tm) mesocrystals are shown in Fig. 2, which exhibit well-defined peaks indicative of highly crystalline and can be well indexed as orthorhombic YbF_3 (JCPDS no. 49-1805), ErF_3 (JCPDS no.32-0361) and TmF_3 (JCPDS no.32-1352) crystal phases, respectively (space group *Pnma*). No diffraction peaks from residues or impurities have been detected, indicating the high purity of the products. The calculated lattice constants of REF_3 (RE=Yb,Er,Tm) are as follows: a = 6.186, b= 6.812, and c= 4.412 Å for YbF_3, a = 6.306, b= 6.883, and c= 4.376 Å for ErF_3, and a = 6.275, b= 6.833, and c= 4.444 Å for TmF_3. Considering the same orthorhombic phase and the similar lattice constants between YbF_3 and ErF_3, Er^{3+} as an activator was incorporated into YbF_3 host lattice and then investigated its luminescence properties.

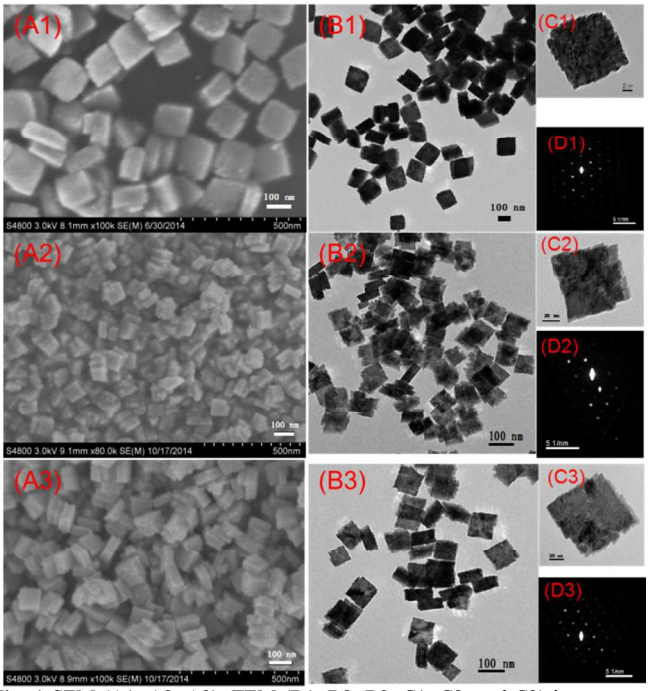

Fig. 1 SEM (A1, A2 ,A3), TEM (B1, B2, B3, C1, C2, and C3) images, and SAED patterns (D1, D2, D3) of REF_3 (RE=Yb,Er,Tm) mesocrystals(A1,B1,C1, and D1 for YbF_3, A2, B2, C2, and D2 for ErF_3, and A3, B3, C3, and D3 for TmF_3, the scale bar in C1, C2 and C3 represents 20 nm, while in other cases 100 nm).

As shown in Fig. 3a, the strong bands at around 3380 and 3310 cm^{-1} due to the –OH stretching vibrations were observed in the IR spectrum of as-synthesized $YbF_3:Er^{3+}$. The peaks located at 1635 cm^{-1} could be assigned to –OH bending vibrations. Free –OH with a stretching frequency at around 3650 cm^{-1} is found to be absent. Careful examination of the IR spectrum shows that on the broad hump (due to –OH stretching vibrations), a small shoulder at 2902 cm^{-1} is present which can be ascribed to stretching vibrations of a $–CH_2$ group of 1,4-butanediol molecules. All these observations support the samples were covered by a large number of hydroxyl groups of 1,4-butanediol which is used as the solvent. Plenty of –OH group on the surface of mesocrystals can form hydrogen bond with water molecules, which rendered excellent dispersibility in water lasting for one weak.[6b,6c] The photograph of YbF_3 mesocrystal dispersed in water is shown in the insert of Fig. 3. It can be seen clearly that the as-prepared YbF_3 mesocrystal can be stably dispersed in water to form colloidal without precipitation for more than one week. After annealed at 350 ℃, the –OH stretching vibration bands vanished (Fig. 3b). In this case, the annealed samples cannot be effectively dispersed in water.

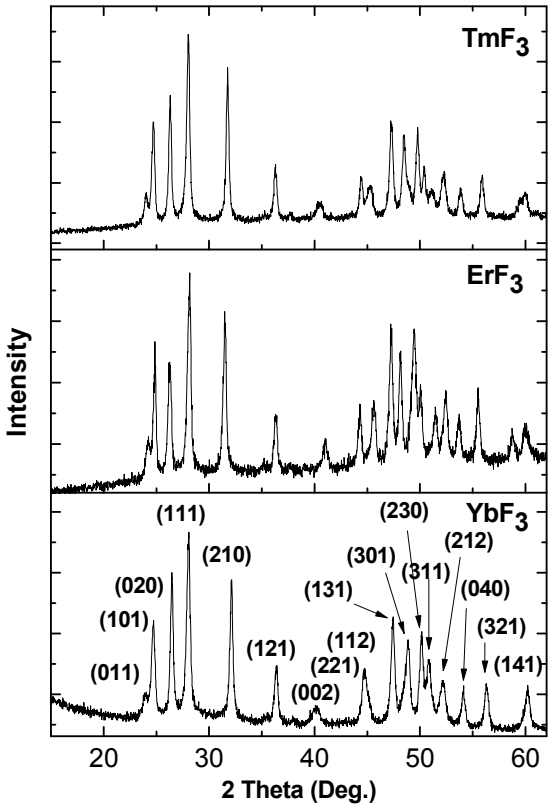

Fig. 2 XRD patterns of REF_3 (RE=Yb,Er,Tm) mesocrystals.

The UC emission spectra of as-synthesized and heat-treated $YbF_3:Er^{3+}$ upon excitation of 980 nm are shown in Fig. 4, respectively. No visible emission (i.e. green and red light) was observed in the as-prepared sample. However, as revealed in Fig. 4(b), the heat-treated sample exhibited green emission peaks at 516/519 nm ($^2H_{11/2} \rightarrow {}^4I_{15/2}$) and 532/541 nm ($^4S_{3/2} \rightarrow {}^4I_{15/2}$) as well as red emission bands centered at 652/662 nm ($^4F_{9/2} \rightarrow {}^4I_{15/2}$).[7] The overall luminescence color is yellow. Obviously, the presence of

high energy –OH group on the surfaces of mesocrtysals prohibited upconversion emission.

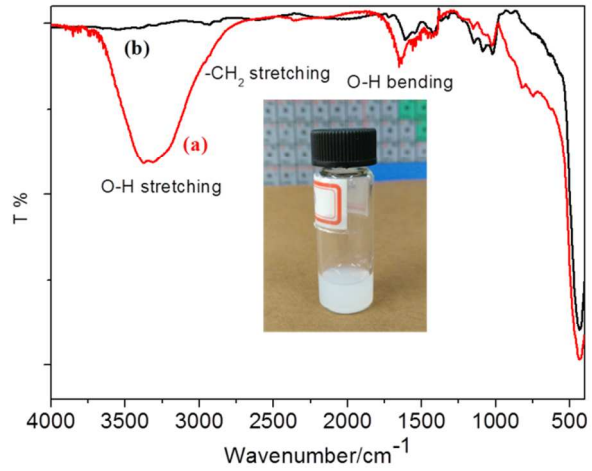

Fig. 3 FT-IR spectra of (a) as-synthesized and (b) heat-treated $YbF_3:Er^{3+}$ (the inset shows the digital photograph of as-synthesized YbF_3 mesocrystal dispelled in water).

Fig. 5 shows NIR emission spectra of $YbF_3:Er^{3+}$(*x* mol%) mesocrystals with various Er^{3+} doping levels upon radiation of 980 nm. A broad emission band extending from 1475 to 1600 nm and centered at 1541 nm was observed and can be attributed to the transition from the first excited state ($^4I_{13/2}$) to the ground state ($^4I_{15/2}$) of the partially filled 4*f* shell of Er^{3+}.[7b,8] NIR emission behavior as a function of Er^{3+} doping concentrations was also investigated. Obviously, the broad band emission feature remains the same on changing doping contents of Er^{3+}. The emission intensity enhances with increasing Er^{3+} content from 1 to 2 mol% and then gradually weakens with further increasing Er^{3+} level to 10 mol%. The decrease of NIR emission intensity can be ascribed to the concentration quenching. And the optimal Er^{3+} doping level was determined to be 2.0 mol%. Hence, in the following work, the doping content of Er^{3+} was fixed at 2 mol%.

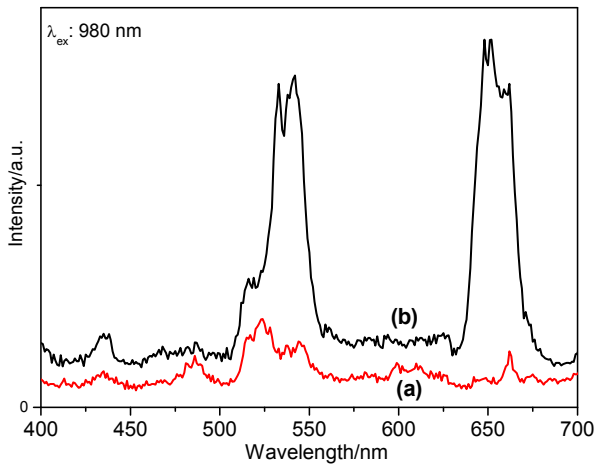

Fig. 4 UC emission spectra of (a) as-synthesized and (b) heat-treated $YbF_3:Er^{3+}$(2 mol%) samples.

As revealed in Fig. S1 of ESI, the addition of Ce^{3+} co-dopant in $YbF_3:Er^{3+}$ with fixed Er^{3+} doping content can improve the NIR emission intensity. NIR emission enhances with the increasing of Ce^{3+} content from 1 mol% to 5 mol%, then following a falling trend. The improved emission intensity with co-doping of Ce^{3+} may be due to the enhanced interactions between Ce^{3+} and Er^{3+}, which increased population density of the Er^{3+} $^4I_{13/2}$ level.[6d] The corresponding compositional analysis of the products using EDS (Fig. S2 of ESI) confirms that the chemical signatures taken within different parts of the sample are identical within experimental accuracy and that the as-obtained samples contain Yb, Ce and F elements (Er or Ce elements were not detected due to their low doing levels). Further details on the electronic transitions of $YbF_3:Er^{3+},Ce^{3+}$ will be discussed in a future publication.

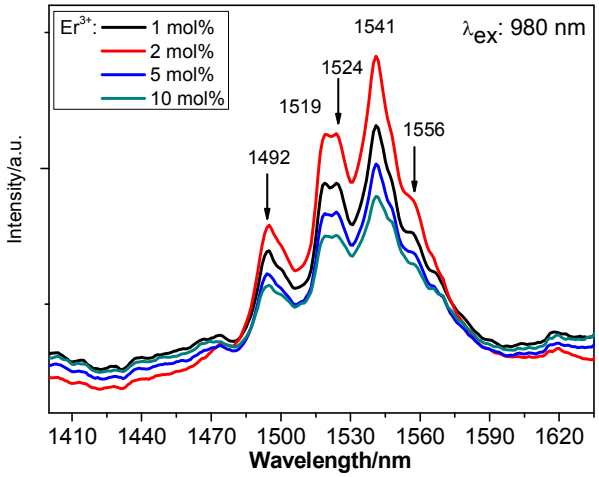

Fig. 5 NIR emission spectra of $YbF_3:Er^{3+}$(*x* mol%) mesocrystals with various Er^{3+} doping levels.

In summary, hydrophilic REF_3 (RE=Yb,Er,Tm) mesocrystals as well as Er^{3+}-/Ce^{3+}- single or double doped analogues were fabricated by an additive-free one-pot solvothermal reaction. Each of nano-plate architecture is composed of many nanoparticles with coarse surface. Er^{3+}-activated YbF_3 mesocrystalline nanophosphor exhibited 1.5 μm near-infrared luminescence but no visible upconversion emission upon 980 nm radiation. The presence of plenty of –OH group anchored on the surfaces renders the excellent dispersion in water and quenches the upconversion luminescence. These properties, combined with the ease of synthesis and high water solubility, make these or related mesocrystal compounds excellent candidates for use in biomedical applications.

Experimental (Bold 11 pts)

Materials

Rare earths oxides RE_2O_3 (RE=Yb,Er,Tm, 4N), 1,4–butanediol (≥ 99%), concentrated nitric acid (HNO_3, ≥ 68.0%), and ethanol (≥ 99.7%) were purchased from Sinopharm Chemical Reagent Co., China. Ionic liquid (IL) 1-butyl-3-methylimidazolium hexafluorophosphate ($BmimPF_6$, 99%) was supplied by Sigma-Aldrich Co., China. All of the chemicals were used as received without further purification. RE_2O_3 powders were separately

dissolved in dilute HNO_3 solution and the residual HNO_3 and water was removed by heating and evaporation, resulting in the formation of corresponding $RE(NO_3)_3{\cdot}xH_2O$.

Synthesis

Hydrophilic rare-earths trifluoride REF_3 (RE=Yb,Er,Tm) mesocrystals were fabricated by hydrothermal treatment of $RE(NO_3)_3$ and $BmimPF_6$ in the presence of 1,4–butanediol. Herein, the required fluoride anions are provided by $BmimPF_6$ as a result of its hydrolysis [10]. Even without additional water, $BmimPF_6$ can hydrolyze with the aid of hydration water molecules from $RE(NO_3)_3{\cdot}xH_2O$ salts [11]. The reaction procedures are given as follows.

$$PF_6^- (IL) + H_2O = PF_5{\cdot}H_2O + F^- \quad (1)$$

$$RE^{3+} + 3F^- = REF_3\downarrow \quad (2)$$

In a typical synthesis, 0.50 mmol $RE(NO_3)_3$ was dissolved in 5.0 mL of 1,4–butanediol under vigorous stirring, heating the vial at ~100 ℃ to facilitate the dissolution process. After the butanediol solution was cooled down to room temperature, it was then transferred into a 25 mL polytetra-fluoroethylene vial containing stoichiometric $BmimPF_6$. The vial was sealed and kept at 120 ℃ for 24 hrs. The final products were collected, washed several times with ethanol and deionic water, and purified by centrifugation. After fully drying at 70 ℃ under dynamic vacuum for 24 hrs, REF_3 (RE=Yb,Er,Tm) powder samples were obtained.

Characterization

X-ray diffraction (XRD) measurements were carried out on a Bruker D8 Advanced X-Ray Diffractometer with Ni filtered Cu Ka radiation (λ = 1.5406 Å) at a voltage of 40 kV and a current of 40 mA. The morphologies of samples were characterized by Field emission scanning electron microscopy (FE-SEM, Hitachi S4800) and transmission electron microscopy (TEM, JEOL-2100F). The selected area electron diffraction (SAED) patterns and energy-dispersive X-ray spectroscopic (EDX) analysis were acquired using TEM (JEOL-2100F), FESEM equipped with an energy dispersive X-ray spectroscope, respectively. Near infared (NIR) emission spectra were obtained on an Edinburgh Instruments FLS920 spectrofluorimeter equipped with a 980 nm laser diode. The spectrum for the sample was recorded from solid samples immobilized on a microscope glass slide. Fourier transform infrared (FT-IR) spectrum analyses were operated on samples pelletized with KBr powder in the range of 4000−400 cm^{-1} using an infrared Fourier transform spectrophotometer (Nicolet, ZOSX). All of the measurements were obtained from powder samples and performed at room temperature.

ACKNOWLEDGMENTS

The authors gratefully acknowledge financial support from Natural Science Foundation of China (Grant No. 91122003) and Developing Science Funds of Tongji University. X. He would also like to thank Natural Science Foundation of China (Grant No. 21373103) for the financial support.

Notes and references

[a] *Department of Chemistry, Tongji University, Shanghai 200092, China. E-mail: byan@tongji.edu.cn*
[b] *School of Chemistry and Environmental Engineering, Jiangsu University of Technology, Changzhou, Jiangsu 213001, China. E-mail: hexh@jsut.edu.cn*

† Electronic Supplementary Information (ESI) available: Experimental details, Fig.S1–S2. See DOI: 10.1039/b000000x/

1 (*a*) Y. Liu, D. Tu, H. Zhu and X. Chen, *Chem. Soc. Rev.*, 2013, **42**, 6924; (*b*) V. Muhr, S. Wilhelm, T. Hirsch, and O. S. Wolfbeis, *Acc. Chem. Res.*, 2014, **47**, 3481.

2 A. Sedlmeier and H. H. Gorris, *Chem. Soc. Rev.*, 2015, 44, 1526.

3 (*a*) G. Chen, H. Qiu, P. N. Prasad, and X. Chen, *Chem. Rev.*, 2014, **114**, 5161; (*b*) S. Gai, C. Li, P. Yang, and J. Lin, *Chem. Rev.*, 2014, **114**, 2343; (*c*) H. H. Gorris and O. S. Wolfbeis, *Angew. Chem. Int. Ed.*, 2013, **52**, 3584; (*d*) C. Liu, Y. Hou, and M. Gao, *Adv. Mater.*, 2014, **26**, 6922.

4 (*a*) N. Bogdan, F. Vetrone, G. A. Ozin, and J. A. Capobianco, *Nano Lett.*, 2011, **11**, 835; (*b*) Z. Chen, H. Chen, H. Hu, M. Yu, F. Li, Q. Zhang, Z. Zhou, T. Yi, and C. Huang, *J. Am. Chem. Soc.*, 2008, **130**, 3023.

5 *(a)* G. Blasse, B. C. Grabmaier, *Luminescent Materials*; Springer Verlag: Berlin, 1994; (*b*) M. Niraj Luwang, R. S. Ningthoujam, Jagannath, S. K. Srivastava, and R. K. Vatsa, *J. Am. Chem. Soc.*, 2010, **132**, 2759.

6 (*a*) M. Haase, and H. Schäfer, *Angew. Chem. Int. Ed.*, 2011, **50**, 5808; *(b)*F. N. Sayed, V. Grover, S. V. Godbole and A. K. Tyagi. *RSC Adv.*, 2012, **2**, 1161; (*c*) J. Wang, S. Bo, L. Song, J. Hu, X. Liu and Z. Zhen, *Nanotechnology*, 2007, **18**, 465606; (*d*) M. C. Tan, G. A. Kumar, R. E. Riman, *Opt. Express*, 2009, **17**,15904.

7 (*a*) Z. Wei, L. Sun, J. Liu, J. Zhang, H. Yang, Y. Yang, and L. Shi, *Biomaterials*, 2014, **35**, 387; (*b*) L. Sun, X. Ge, J. Liu, Y. Qiu, Z. Wei, B. Tian and L. Shi, *Nanoscale*, 2014, **6**, 13242.

8 (*a*) J.-C. G. Bünzli, and S. V. Eliseeva, *J. Rare Earths*, 2010, **28**, 824; (*b*) H. Q. Ye, Z. Li, Y. Peng, C. C.Wang, T. Y. Li, Y. X. Zheng, A. Sapelkin1, G. Adamopoulos, I. Hernández, P. B.Wyatt and W. P. Gillin, *Nat. Mater.*, 2014, **13**, 382; (*c*) Q. Xiao, H. Zhu, D. Tu, E. Ma, and X. Chen, *J. Phys. Chem.*, C 2013, 117, 10834; (*d*) M. V. Vijaya Kumar, K. Rama Gopal, R.R.Reddy, G. V. Lokeswara Reddy, B. C. Jamalaiah, *J. Lumin.*, 2013, **142**, 128; (*e*) B. van Saders, L. Al-Baroudi, M. C. Tan, and R. E. Riman, *Opt. Mater. Express*, 2013, **3**, 566; (*f*) J. Suresh Kumar, K. Pavani, M. P. F. Graca, M. J. Soares, and M. A. Valente, *Phys. Status Solidi (b)*, 2013, **250**, 837.

9 (*a*) H. Cölfen, M. Antonietti, *Angew. Chem. Int. Ed.*, 2005, **44**, 5576; (*b*) M. Niederberger, and H. Cölfen, *Phys. Chem. Chem. Phys.*, 2006, **8**, 3271; (*c*) R. Q. Song, and H. Cölfen, *Adv. Mater.*, 2010, 22,1301; *(d)* L. Zhou, and P. O'Brien, *J. Phys. Chem. Lett.*, 2012, **3**, 620;(*e*) X. He, and B. Yan, *CrystEngComm*, 2015, **17**, 621.

10 (*a*) R. P. Swatloski, J. D. Holbrey and R. D. Rogers, *Green Chem.*, 2003, **5**, 361; (*b*) C. Zhang, J. Chen, Y. C. Zhou and D. Q. Li, *J. Phys. Chem. C*, 2008, **112**, 10083; (*c*) C. Zhang and J. Chen, *Chem. Commun*., 2010, **46**, 592.

11 N. Xie and W. L. Luan, *Nanotechnology*, 2011, **22**, 265609.

